2017

The Compartmented Alginate Fibres Optimisation for Bitumen Rejuvenator Encapsulation

Amir Tabakovic
Technological University Dublin, amir.tabakovic@dit.ie

Dirk Braak
Delft University of Technology

Mark van Gerwen
Delft University of Technology

Oguzhan Copuroglu
Delft U

Wouter Post
Delft University of Technology

See next page for additional authors

Recommended Citation

Tabaković, A.; McNally, C.; Fallon, E., 2016, "Specification development for cold in-situ recycling of asphalt", Journal of Construction and Building Materials, Vol.102, 1, pp.318 – 328. doi.org/10.1016/j.conbuildmat.2015.10.154

The compartmented alginate fibres optimisation for bitumen rejuvenator encapsulation

Abstract

This article presents development of a novel self-healing technology for asphalt pavements, where asphalt binder rejuvenator is encapsulated within the compartmented alginate fibres. The key objective of the study was to optimise the compartmented alginate fibre design, i.e. maximise amount of rejuvenator encapsulated within the fibre. The results demonstrate that optimum rejuvenator content in the alginate fibre is of 70:30 rejuvenator/alginate ratio. The fibres are of sufficient thermal and mechanical strength to survive harsh asphalt mixing and compaction processes. Furthermore, results illustrated that Zeer Open Asfalt Beton (ZOAB) asphalt mix containing 5% of 70:30 rejuvenator/alginate ratio compartmented alginate fibres has higher strength, stiffness and better healing properties in comparison to the control asphalt mix, i.e. mix without fibres, and mixtures containing fibres with lower rejuvenator content. These results show that compartmented alginate fibres encapsulating bitumen rejuvenator present a promising new approach for the development of self-healing asphalt pavement systems.

Key Words: Self-healing, Asphalt pavements, Compartmented fibres, Calcium Alginate, Rejuvenation.

Highlights:

i. 70:30 rejuvenator/alginate ratio is an optimal fibre design mix.
ii. Fibres successfully heals the damage (closes the crack) in asphalt bitumen and mortar mix.
iii. ZOAB asphalt mix containing fibres outperforms the control asphalt mix.
iv. Higher amount of fibres in the mix (>10%) reduce ZOAB asphalt mix stiffness and strength recovery.

1. Introduction

The emergence of self-healing technologies [1] for asphalt pavements signified a turning point in the 250 year evolution of the road (see Figure 1). Previously, changes in road design were driven by industrial innovation (e.g. the invention and mass production of the motor car), to facilitate trade or in response to environmental concerns. The drive to incorporate self-healing technology into road design stems from the concept of the ‘Forever Open Road’, the

need to avoid the traffic disruption caused by road maintenance activities on busy roads. The globally road network spans 16.3 million km [2], of which 5million km is in EU, 4.4milion km is in USA and 3.1million km is in China. These road networks fulfil major economic and social goals by facilitating the movement of goods and people across the globe. The operational health of the road network is of the utmost importance for economic and social life of every region of the globe [3]. As a result governments invest heavily in the development of national road networks, e.g. in 2011 EU governments collectively invested €20billion in the development and maintenance of the EU road network [4]. The ongoing importance of roads as a means of transportation, drives the need for improved road materials and road pavement design.

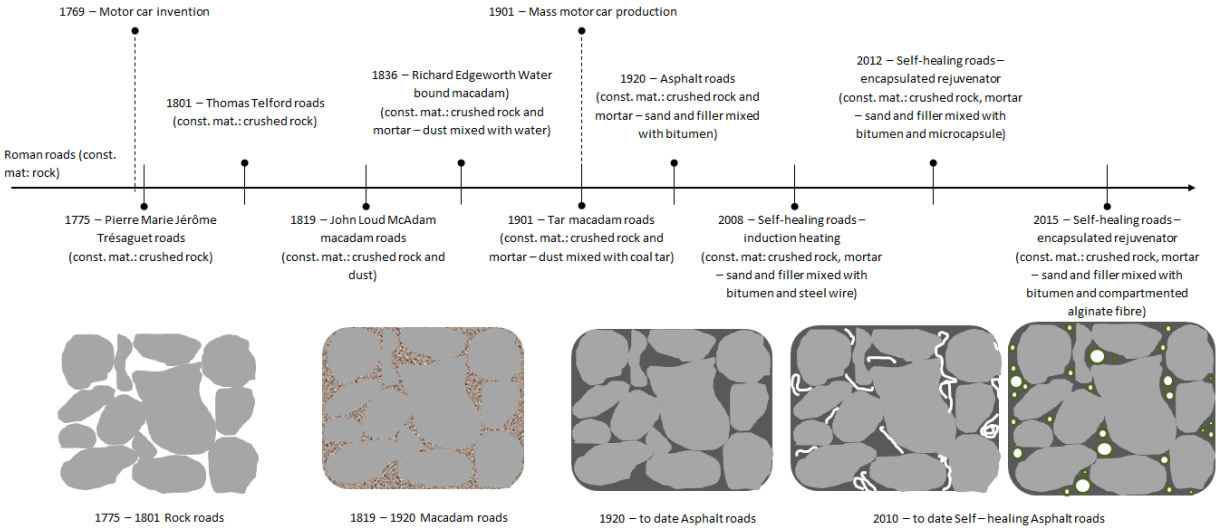

Figure 1 The development of road materials: past, present and future[5-8].

Modern roads are sophisticated engineering creations. Despite this, the materials used to construct them, (bitumen and rock aggregate), haven't changed in over a century. Figure 2 shows the heterogeneous composition of the asphalt pavement mix commonly used today.

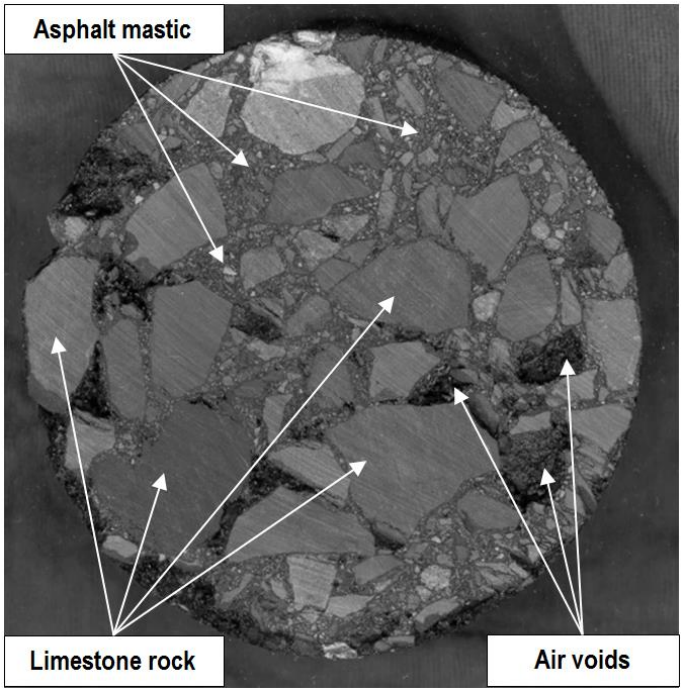

Figure 2 Composition of an asphalt test sample.

The mix is comprised of rock aggregate and binding material or 'mastic' which is composed of fine aggregates (sand and filler) and bitumen , a crude oil (fossil fuel) by-product. Mastic plays an important role in this system as it binds the rock skeleton in place, thereby preventing its disintegration. Unfortunately, environmental factors (rain, snow and ice) and traffic loading conditions can cause bitumen, the main ingredient of the mastic, to age and lose its flexibility. This enables cracks to form within the road pavement and ultimately results in the failure of the pavement system. To the naked eye this would appear as a pothole which at present would require on-site maintenance and disruption to traffic flow.

The challenge for road engineers is to develop a sustainable asphalt mixtures that reduce the likelihood of pavement system failure by developing new road materials and new methods of road construction and maintenance. Progress in the road material science has lagged behind materials, such as concrete and composite materials, likely as a result of the continued availability of low cost materials and due to the functional design of asphalt pavements. Since the 1970s, the focus of the road innovation was to develop more sustainable technologies, for road pavements, e.g. recycled asphalt pavements [9]. Although these innovations served to reuse construction aggregate and old bitumen and reduce the CO_2 footprint of road construction [10], road material design remained unchanged. Other innovative technologies have had unanticipated side effects, so warm asphalt recycling and cold emulsion recycling technologies involve adding chemical additives to lower the asphalt

mixing temperature [9]. Although they reduce the amount of CO_2 in atmosphere, leaching has occurred, where pollutants leach into the ground, posing a contamination threat to soil and to groundwater. Trombulak and Frissell [11] published a damning report on the ecological effects of road construction on terrestrial and aquatic communities. There is growing pressure on the road industry to minimise its environmental impact. There is also a desire to adopt 'Forever Open Road' concept, i.e. improve pavement materials and design in order to reduce road maintenance and improve safety levels for road users. Since 2008, the incorporation of self-healing technology into asphalt pavements has been advancing. Self-healing technology offers an alternative method for road maintenance, where the damage is repaired by an internal (implanted) healing system. The objective of self-healing technology is to enable/assist material systems to heal after damage on a local or global scale. It aims to reduce the local or global level of damage and to extend or to renew the functionality and life-time of the damaged part, system or device. Fisher [12] defines the self-healing and self-repair of a material or system as: "*the ability to substantially return to an initial, proper operating state or condition prior exposure to a dynamic environment by making the necessary adjustments to restore to normality and/or the ability to resist the formation of irregularities and/or defects*".

To date researchers have tested two self-healing methods for asphalt pavements [13-15, 5, 6, 16-19]:

i) Induction heating, electrically conductive fillers (steel fibres and steel wool) were added to the asphalt mix. Healing is initiated within the asphalt by sending an alternating current through the coil and generating an alternating electromagnetic field. When the conductive asphalt specimen is placed beneath the coil, this electromagnetic field induces currents flowing along the conductive loops formed by steel fibres [13]. The current causes steel fibres to heat up which heats the aged bitumen and softens it, allowing it to flow and close the cracks, and to repair the damage. This method can be repeated if damage returns.

ii) Rejuvenation, an encapsulated healing agent (rejuvenator) is added into the asphalt mix to restore the original binder properties. When micro cracks begins to form within the pavement system, they encounter a capsule in the crack propagation path. The fracture energy at the tip of the crack opens the capsule, releasing the healing agent which then diffuses within the asphalt binder to seal the crack.

The rejuvenator encapsulation approach represents a more favourable method of self-healing as it allows for the rejuvenation of aged binder, i.e. enables it to return it to its original

chemical, physical and mechanical properties. Researchers have demonstrated[20, 15-18, 21-23] that various types of capsules containing rejuvenator can be produced and that these capsules are sufficiently thermally and mechanically stable to survive the asphalt production process. However, a difficulty with this approach is that large amounts of microcapsules are needed to make the process effective. The addition of large quantities of microcapsules into the asphalt mix can reduce the quality of the pavement which itself may cause premature pavement failure. Garcia et al. [23, 24] and Sun et al. [22] reported that asphalt stiffness was reduced when microcapsules were added. They explained that softening of asphalt binder (viscosity reduction) was caused by the rejuvenator release. However, it is well documented [25, 26] that deformation in the asphalt mix is caused by sand granulates. It is possible that the inclusion of microcapsules, sand like particles, has also contributed to increased asphalt mix deformation, i.e. rutting. Furthermore, the chemical compounds used in the production of microcapsules, such as melamine–formaldehyde [27], in large quantities could pose an environmental threat via leaching.

The encapsulation of rejuvenator in alginate-based compartmented fibres is explored here as a solution to these problems in asphalt mixtures. Authors previously reported a concept where compartmented alginate fibres encapsulating rejuvenator was tested as self-healing technology for asphalt pavements [8]. The study showed that alginate fibres have great potential as self-healing technique for asphalt pavements, i.e. they can be inserted into the asphalt mastic mix (fibres can survive asphalt mixing and compaction process) and can increase asphalt mastic mix strength by 36%. However, the study showed that fibres have limited healing capacity. The fibres are effective in healing of micro cracks, however the system is less efficient in healing of large cracks. This is due to the small amount of rejuvenator encapsulated in the fibres and available for the healing process. Therefore this study has focused on the optimisation of the compartmented alginate fibre encapsulating the asphalt binder rejuvenator. The study aimed to increase rejuvenator content in the fibre without compromising its physiological, thermal and mechanical properties. A series of compartmented alginate fibres containing varying rejuvenator content has been produced and tested. A special testing programme was designed where physiological properties of the fibres were investigated. The size and volume of encapsulated rejuvenator in each compartment was determined, and as such amount, volume, of rejuvenator per gram of fibre is calculated. These findings allow determination of the exact amount of rejuvenator available for bitumen damage (crack) healing in the test specimen. The effect of the temperature (both low and high) on the mechanical properties of the fibre is investigated. Furthermore, the ability of the self-healing

system to release rejuvenator and heal the crack was investigated by imbedding the fibres in microscopic bitumen and mastic test specimens in which artificial cracks were inserted using a surgical knife. The healing process was recorded using the optical microscope technique. Finally, effect of the fibre in an asphalt mix (Zeer Open Asfalt Beton - ZOAB) was studied, for this study standard Indirect Tensile Stiffness Modulus (ITSM) and Indirect Tensile Strength (ITS) tests were implemented. self-healing

2. Materials and Methods

2.1 Materials and production processes

2.1.1 Compartmented Alginate Fibres Production

The compartmented fibres were spun from an emulsion of rejuvenator suspended in a water solution of sodium alginate. To this aim a 6 wt.% solution of sodium alginate in de-ionized water was prepared. At the same time a 2.5 wt.% poly(ethylene-alt-maleic-anhydride) (PEMA) polymeric surfactant solution was prepared by dissolving the copolymer in water at 70^{o}C and mixing it for 60min. After the PEMA has been dissolved in the water it was allowed to cool to room temperature (20±2^{o}C) and was combined with rejuvenator, forming a healing agent solution, in PEMA/rejuvenator 1/1.5 proportion. Sodium alginate and PEMA/rejuvenator solutions were then combined in six varying rejuvenator/alginate proportions, the proportions are given in the Table 1. All of the solutions were mixed at 200rpm for 60 seconds. It is important to note that the stirring rate and stirring time can be used to control the size of the rejuvenator droplets in the solution and thus the size of the rejuvenator compartments [6, 28, 8]. If the stirring rate is low and stirring time is short, the droplets will be larger, but if the stirring rate is high and the stirring time is long, the droplets will be smaller.

Table 1 Summary of the rejuvenator/alginate ratios

Material	Ratios (%)					
	0:100	40:60	50:50	60:40	70:30	80:20
Rejuvenator (g)	0	1.5	2.2	3.1	4.5	6.9
Alginate (g)	2.4	2.5	2.2	2.1	1.9	1.7

The emulsions were spun with a plunger-based lab scale wet spinning line in a conventional wet spinning process [28, 29, 8] to form the rejuvenator-filled compartmented fibres. More details on the fibre preparation and spinning process can be found elsewhere [29]. All

chemicals used in the process were purchased from Sigma Aldrich, The Netherlands, except rejuvenator, Modesel R20, which was provided by Latexfalt B.V..

2.1.2 Porous Asphalt mastic mix design and mixing procedure

In an effort to evaluate the efficiency of rejuvenator encapsulated in compartmented aclcium alginate fibres, a ZOAB asphalt mix was designed. The grading envelope according to the Rationalisatie en Automatisering Grond-, Water- en Wegenbouw (RAW) 2015 was used in effort to produce ZOAB asphalt mix typically used as asphalt wearing courses used in the Netherlands [30, 31]. Limestone originates from a quarry in Norway, the filler material is hydrated lime (Wigro 60K) and for bitumen, pen 70/100 was used in this research. Figure 3 illustrates the mix grading curve, the figure shows good fit of the mix with in grading envelope. The figure shows slightly higher passing of the fin material than required by the grading limits, however as the aggregate contained high content of dust it was impossible to achieve 100% fit. Further consultations with industrial partners confirmed that the fit is suitable for ZOAB mix production. Table 2 summarises these mix constituents and shows their proportions in the mix with and without fibres. The fibre are added in amount of 5% and 10% of total bitumen content in the mix, which in total mix volume it represents 0.23% and 0.45% respectively. The aggregate mix constituent content was not changed with insertion of the fibres in the mix.

Table 2 ZOAB mix design, (percentage constituent content is given by weight).

Mix Constituent	% content in mix		
	without fibres	5% fibres	10% fibres
C22.4	20.1	20.1	20.1
C16.0	25.6	25.6	25.6
C11.2	34.8	34.8	34.8
C8.0	7.4	7.4	7.4
C6.0	6.7	6.7	6.7
Sand (2.0)	0.5	0.5	0.5
Filler (<0.063)	0.5	0.5	0.5
Bitumen	4.5	4.3	4.1
Fibre	0	0.23	0.45

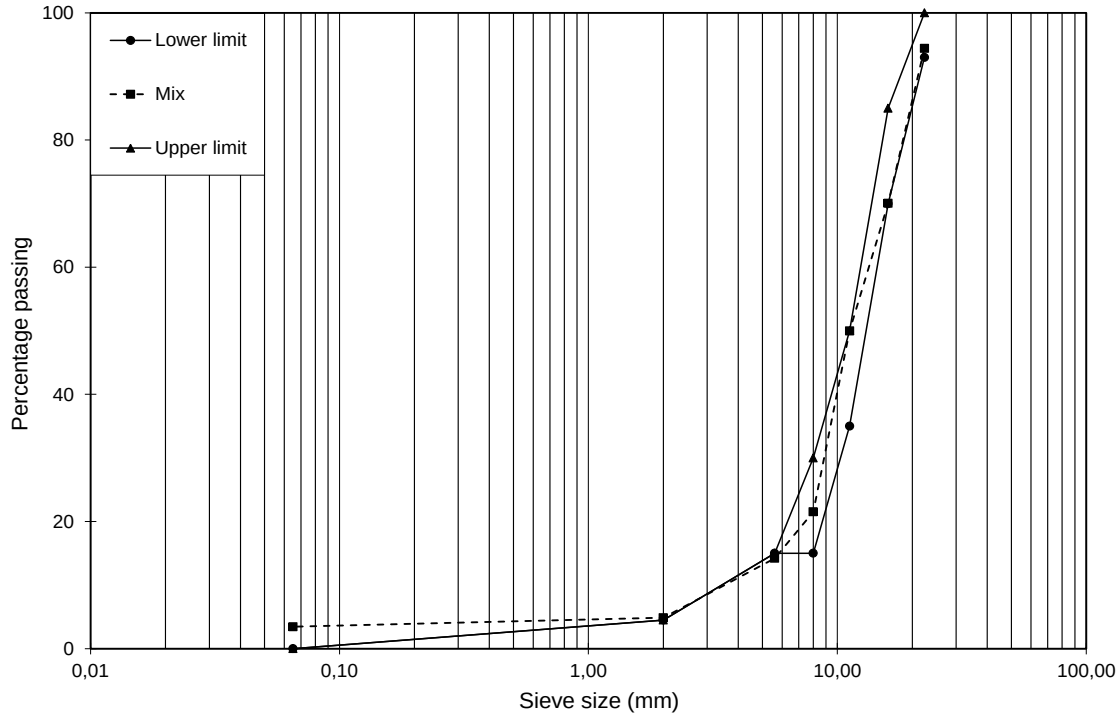

Figure 3 Porous asphalt mix grading, grading envelope RAW 2015 [32].

The porous asphalt mix was prepared using a 5l Hobart mixer. Prior to mixing, all mix constituents were preheated to 160^{o}C for 2 hours. During the mixing process sand, filler and bitumen were mixed first, fibres were gradually added to the mix in order to avoid conglomeration of fibres within the mix. The fibres were gradually inserted into the mastic mix which resulted prolonged asphalt mixing period causing the mix to cool down and reduce its workability. Therefore, the mix had to be reheated several times at 160^{o}C. The final mixing was performed by hand, in order to ensure that the mix constituents (sand, filler and fibres) were fully and evenly coated by the bitumen.

In order to account for the asphalt field ageing effect an ageing programme was developed. The ageing programme consisted of a protocol:

- Long term; 15 years filed ageing 4 hours at 135^{o}C followed by 4 days at 85^{o}C in forced air draft oven.

The ageing protocol was adopted from Kliewer et. al. [33]. Recently Tabaković et al. [8] and Casado Barrasa et. al. [34] successfully used a similar protocol to investigate the effect of short and long term ageing of the asphalt mix containing alginate capsules and microcapsules encapsulating asphalt binder rejuvenator.

After asphalt ageing procedure the fibre were added to the mix. Prior to the fibre inclusion into the mix, the mix was preheated to the standard asphalt mixing/compaction temperature

160°C [35]. The fibres were then gradually added to the mix in order to avoid conglomeration of fibres within the mix. After the fibre inclusion into the mix the test specimens were prepared.

The test specimens were compacted in accordance with IS EN 12697-31:2007 using a SERVOPAC gyratory compactor. The static compaction pressure was set at 0.6MPa with an angular velocity of 30 gyrations per minute and the gyratory angle set at 1.25°. A set number of gyrations are used as the compaction control target, in this case 100 gyrations. For this study the cylindrical test specimens are compacted to target dimensions of 100mm in diameter and 50mm in height. After compaction, test specimens are left in the mould to cure for 2 hours. The test specimens are then extruded, and their dimensions and weight recorded.

2.2 Fibre and composite characterization

2.2.1 Optical microscopy

A Leica 2500P polarised light microscope was used to observe the rejuvenator release from the fibre compartments, its capillary flow and consequent damage repair (crack closure) over time. A microscopic image of each fibre test sample was acquired with a Leica DFC310FX digital camera at 1392 × 1040 uninterpolated resolution for image analysis and publication. Following the previous work done by [8], a sample was prepared by placing an alginate fibre containing rejuvenator capsules onto the object glass. The bitumen and asphalt mastic mix was placed on top of the fibres An artificial incision was made in the binder/asphalt mastic matrix and fibre using a surgical scalpel. The software Leica LAS Live Image Builder was used to record the rejuvenator release and its capillary flow.

2.2.2 Environmental Scanning Electron Microscope (ESEM)

The Environmental Scanning Electron Microscope (ESEM) was used to evaluate the morphology of the rejuvenator compartments within the sodium alginate fibres. For this purpose, a Philips XL30 ESEM system was employed. Low accelerating voltage of 10kV and a beam current of less than 1nA were used to limit the electron beam damage on the heat sensitive polymeric fibres.

2.2.3 Fibre thermal conditioning

In order to investigate temperature effect on the mechanical properties, tensile strength, of the fibres a special thermal conditioning tests was developed. Where the fibres were subjected to a thermal conditioning at varying temperatures, of: 20°C and between 80°C – 160°C, in steps of 20°C, using standard draft oven. Fibre samples were placed in the oven at set temperature for duration of 15minutes. After thermal conditioning fibres were taken out of the oven and

left to condition to the test temperature of 20 ± 3°C for additional 15 minutes. Due to the low mass of the fibre samples it has been assumed that 15 minutes would be sufficient time for the fibre to condition to the desired temperature. As well as high temperature, fibres were subjected to the low (8.5°C) and freezing (-18.5°C) temperature. For cold fibre conditioning, laboratory fridge and freezer were used. The conditioning and test pre-conditioning times were also 15 minutes.

2.2.4 Uniaxial Tensile Test (UTT)

The tensile strength of the rejuvenator-containing alginate fibres was determined using a micro tensile testing machine with 500N load cell and at a cross-head speed of 0.01mm/s. Fibres (cut from a continuous filament of approximately 20m long) were glued onto supporting brass plates with a gauge length of 10mm accordingly. A batch of 10 fibres of each mix ratio were tested successfully. The fibre strain was measured from the machine cross-head displacement taking into account the system compliance.

2.2.5 Thermogravimetric analysis (TGA)

The thermal stability characterizations of Sodium Alginate fibres containing varying rejuvenator/alginate ratios were performed using NETZSCH STA 449 F3 Jupiter TGA system, at a scanning rate of 6.5°C/min in Argon gas (Ar) at flow of 50 ml/min.

2.3 Porous asphalt performance

2.3.1 Indirect Tensile Stiffness Modulus (ITSM) test

The non-destructive ITSM test is conducted, which complied with IS EN 12697-26: 2012. The Universal Testing Machine (UTM) with a pneumatic close loop control system is used. Two linear variable differential transformers (LVDT) were used to measure the horizontal deformation. The specimens were conditioned at 20°C, for four hours prior to testing. The stiffness value was recorded on two diameters orientated at 90° to each other, and an average of these two values was reported as the specimen stiffness.

2.3.2 Indirect tensile strength test

On completion of the ITSM test, the specimens were stored in a temperature control chamber at 20°C and left to condition for an hour prior to testing. The UTM testing system is employed to complete the Indirect Tensile Strength Test (ITS) in accordance with EN 12697-23: 2003. The ITS test is conducted by applying a vertical compressive strip load at a constant loading rate, in this case 0.1mm/s, to a cylindrical specimen. The load is distributed over the thickness

of the specimen through two loading strips at the top and bottom of the test specimen. The tests were conducted at a temperature of 20^{o}C.

2.3.3 Healing efficiency of the ZOAB asphalt mix containing fibres

In order to investigate effect of the fibres on mechanical properties of the asphalt mix and evaluate the healing efficiency of the compartmented fibres encapsulating the rejuvenator, a special testing programme was designed:

1. Two fibre amounts 5% and 10%,
2. Tests, ITSM and ITS,
3. Test temperature 20^{o}C,
4. Healing temperature 20^{o}C,
5. Healing time 20 hours and 40 hours after initial test.

The testing protocol was to as follows:

1. Test samples test temperature pre-conditioning,
2. ITSM test diameter I followed by diameter II,
3. Test specimen relaxation 2h, followed by 1st ITS test,
4. Positioning test specimen into healing ring and healing for 2h,
5. ITSM repeat – post ITS test,
6. Positioning test specimen into healing ring and healing for additional 18h,
7. ITSM test - pre 2nd ITS test,
8. 2nd ITS test,
9. Positioning test specimen into healing ring and healing for additional 20h,
10. ITSM test - pre 3rd ITS test,
11. 3rd ITS test.

3. Results and Discussion

3.1 Fibre Composition and morphology

The optical light microscope and ESEM technique were employed in order to conduct volumetric analysis of the fibres. Using the light microscope, thelongitudinal size of the fibre compartments were measured. Figure 4 shows the image of all six fibre rejuvenator/alginate ratios, with a field of view of approximately 3mm. In the Figure 4 the increase of the compartment size can be observed with increase of the rejuvenator volume in the fibre. Here, the ratio 80:20 shows near hollow fibres, i.e. fibre with very large rejuvenator compartments.

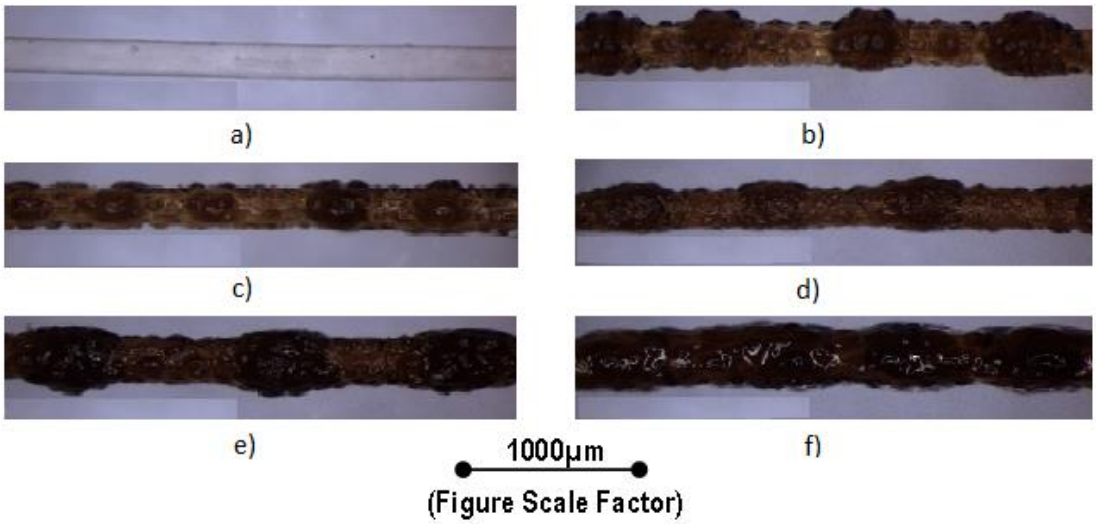

Figure 4 Light optical microscope images of compartmented fibres of varying rejuvenator/alginate ratios; a) 0:100, b) 40:60, c) 50:50, d) 60:40, e) 70:30 and f) 80:20.

The ESEM microscopic analysis technique was employed to analyse cross sectional area of the fibres. The ESEM allows larger magnification of the fibres, which is necessary for the observation of the fibre walls. For this analysis three test samples of each fibre rejuvenator/alginate ratio were used. Figure 5 shows the cross sectional area of the two fibres samples, a)40:60 and b) 60:40 – rejuvenator/alginate ratio, viewed through the ESEM.

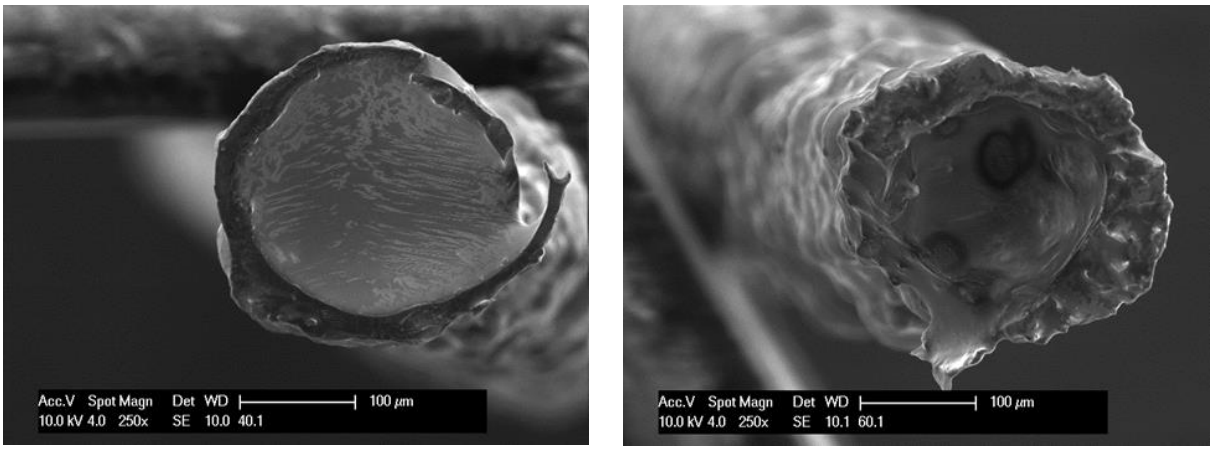

a) b)

Figure 5 ESEM images of the fibre compartment cross section, rejuvenator/alginate ratio; a) 40:60 and b) 60:40.

Volumetric analysis of the fibre compartments were conducted by analysing the microscopic images. The microscopic images were further studied using the ImageJ software [36]. For this analysis it was assumed that all compartments resemble an ellipsoid. The images were imported into the ImageJ software and using its geometry tools, the geometry of the

compartments, the minimum and maximum diameters of all ellipsoids, were recorded. Next step in the volumetric analysis of the fibres was the fibre compartment wall/shell thickness analysis. For this, the images of the fibre cross section were taken with the ESEM and were then analysed with ImageJ using the BoneJ plugin [37]. This plugin has been developed and used for the bone structure analysis. However, it can also be employed for analysis of different structures, in this case of the alginate fibres compartment walls/shell. Using BoneJ the mean wall thickness of every fibre was determined and a thickness map, displaying the thickness throughout the cross-section, was computed. Figure 6 shows an ESEM image of a cross-section and the BoneJ thickness map.

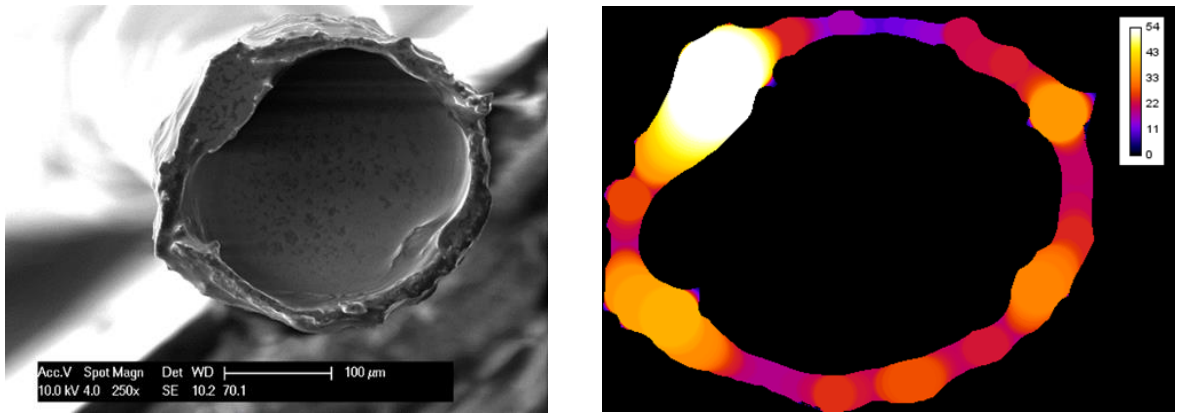

a) b)

Figure 6 Fibre compartment cross sectional analysis; rejuvenator/alginate ratio 70:30. a) ESEM image of the fibre compartment cross section and b) BoneJ fibre compartment wall/shell thickness map.

The results presented in Table 3 show large standard deviations for fibre types except the fibre with a 70:30 rejuvenator/alginate ratio. This was expected because of the relatively small number of samples analysed. These, results show that the wall thickness of the 70:30 ratio is very consistent which is positive and also leads to more accurate volume calculations. The results further show that the 60:40 ratio has the thickest walls which is not expected as it contains less alginate than the ratios 40:60 and 50:50. The thinnest walls are found in the 70:30 ratio.

Table 3 Fibre wall/shell thickness

Ratio	Mean wall thickness (µm)	Wall thickness standard deviation (µm)	Median of compartment volume corrected for wall thickness (µL)
40:60	36.23	10.40	0.0037
50:50	42.84	7.01	0.0014
60:40	55.38	9.01	0.0024
70:30	33.05	1.82	0.0162
80:20	36.13	14.72	0.0139

To calculate the volume of the compartments the mean wall thickness is subtracted from the previously determined ellipse volume. The median is calculated for all the volumes of every fibre ratio. The median is used in order to obtain more accurate results for the fibre compartment volume. Where test sample, using the median to obtain average value of the fibre compartment wall thickness extreme values have less of an effect on the average volume size then using the mean value. As the sample size was small in comparison to the fibre length the extremes have a significant effect on the calculated volume if the mean is used. The medians of the volume of rejuvenator per ratio are presented in Table 4. The lowest volume is found in the 50:50 samples and the highest volume is found in the 70:30 samples. A substantial difference is observed for the fibre volumes of the 70:30 and 80:20 ratios, in comparison to the other ratios. It was expected that the 80:20 ratio would contain the most rejuvenator but results indicated otherwise. This can be explained by the fact that the 80:20 batch is the max rejuvenator/alginate ratio for the fibre production, as such there was not enough alginate within the solution to encapsulate all the rejuvenator and also post fibre production it was observed that rejuvenator was leaking from the fibre indicating the collapse of the fibre compartments.

In order to calculate the volume of rejuvenator per unit length of fibre the median number of compartments is calculated, for each fibre type (rejuvenator/alginate ratio) from the optical microscope images. This data was combined with the median volumes of the compartments and results in a volume of rejuvenator per unit length of fibre, the results are presented in Table 4. The results show that the 50:50 fibre contains the most compartments per 10mm, but since it contains only a low volume per compartment the total volume per 10mm is still the lowest of all the fibre types. The ratio 70:30 contains the most rejuvenator per 10mm closely followed by the 80:20 fibre type. The differences between these two fibre types compared to the other ones are substantial as the compartments are approximately 3-6 times bigger.

In order to relate the fibre compartment volume to the weight of the fibres samples with a length of one meter have been weighed and the average weight per 10mm was calculated. Subsequently the volume per gram of fibre could be calculated using the results in Table 4. The results show that the 70:30 ratios contain the most rejuvenator per gram. The 50:50 fibre contains the least amount of rejuvenator.

Table 4 Compartmented alginate fibre volumetric data.

Ratio	Median number of compartments per 10mm	Compartment volume per 10mm of fibre (µL)	Weight of fibre per 10mm (mg)	Volume of compartment (rejuvenator) per gram of fibre (µL)
40:60	13.90	0.052	0.354	145.7
50:50	20.62	0.028	0.440	64.5
60:40	15.67	0.037	0.487	75.8
70:30	10.47	0.170	0.444	382.9
80:20	10.47	0.146	0.594	245.7

3.2 Thermo-mechanical stability of the fibres

Figure 7 summarises the results of the uniaxial tensile strength (UTS) test used to investigate temperature effect on the fibre strength. The results from the graph show that fibres with higher rejuvenator and lower alginate content have lower values for UTS. Whereas control fibres, without rejuvenator (rejuvenator/alginate ratio of 0:100), have the highest UTS for all temperatures tested. This could be due to the two reasons: i) the pure alginate fibre does not contain large rejuvenator compartments, i.e. it has uniform cross section area, which results in higher strength and ii) loss in moisture in the fibre making it more brittle, so the stress increases but the strain decreases. The UTS of the 70:30 fibres shows to be at the lower end, in the range between 20 and 53 MPa depending on the conditioning temperature. However, its linearity, small change in UTS across the thermal range, indicates the small effect of temperature (high and low) on the fibre properties. From the results it can be seen that a higher rejuvenator content produces a more linear distribution of the UTS, due to the uniformity of the compartment geometry.

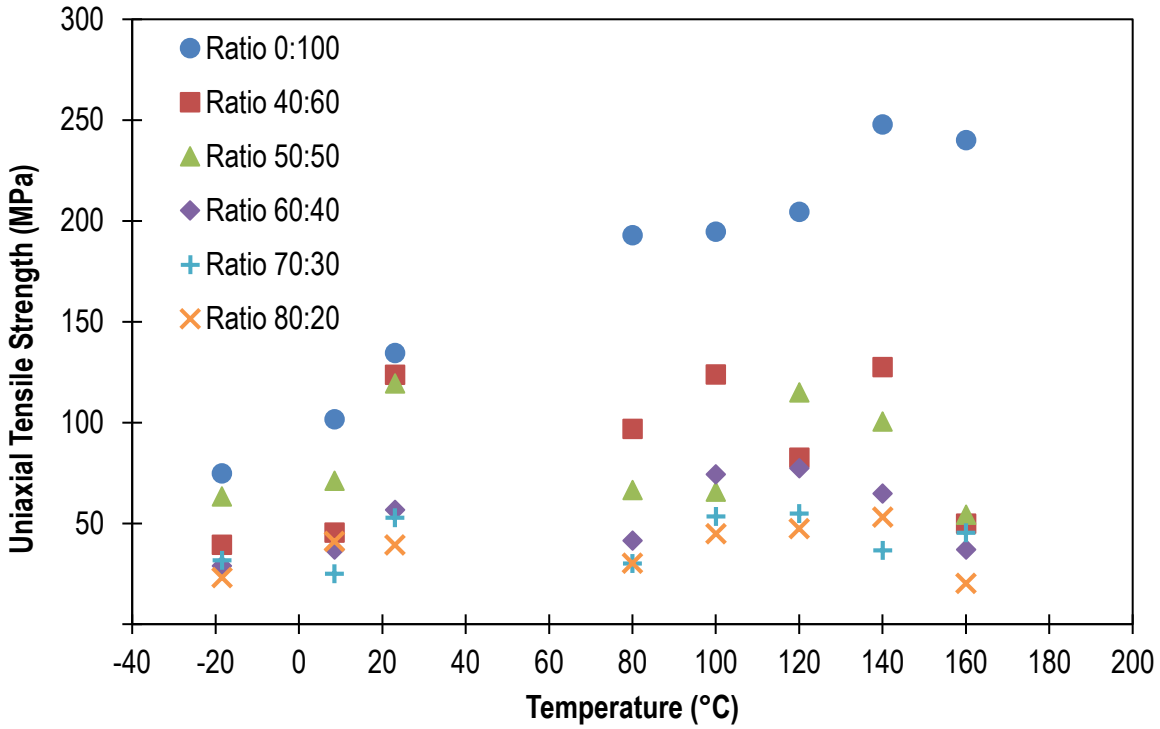

Figure 7 Fibre UTS vs Temperature graph

Figure 8 illustrate the results of the TGA analysis. The results shows that the fibres containing lower amounts of rejuvenator lose more mass, this is due higher moisture content which is contained in the calcium alginate [8]. Table 5 summarises mass loss for every fibre ratio at 160 °C. The results show that fibre with 40:60 rejuvenator/alginate ratio experiences the highest mass loss, at 160 °C. Where, the 80:20 fibre containing the highest rejuvenator content loses the least amount of mass, at temperature of 160 °C. The results clearly shows that a higher rejuvenator content leads to less mass being lost which confirms that the fibre mass loss is due to the residual water evaporation from the calcium alginate. The results further show that compartmented fibres lose between 15% and 30% of their weight at 300°C, whereas fibre without rejuvenator compartments, control fibre of rejuvenator/alginate ratio 0:100, loses at >40% of its weight at 300°C. These results indicate that the alginate fibre encapsulating rejuvenator can, in principle, resist the high processing temperatures of the asphalt mixing process.

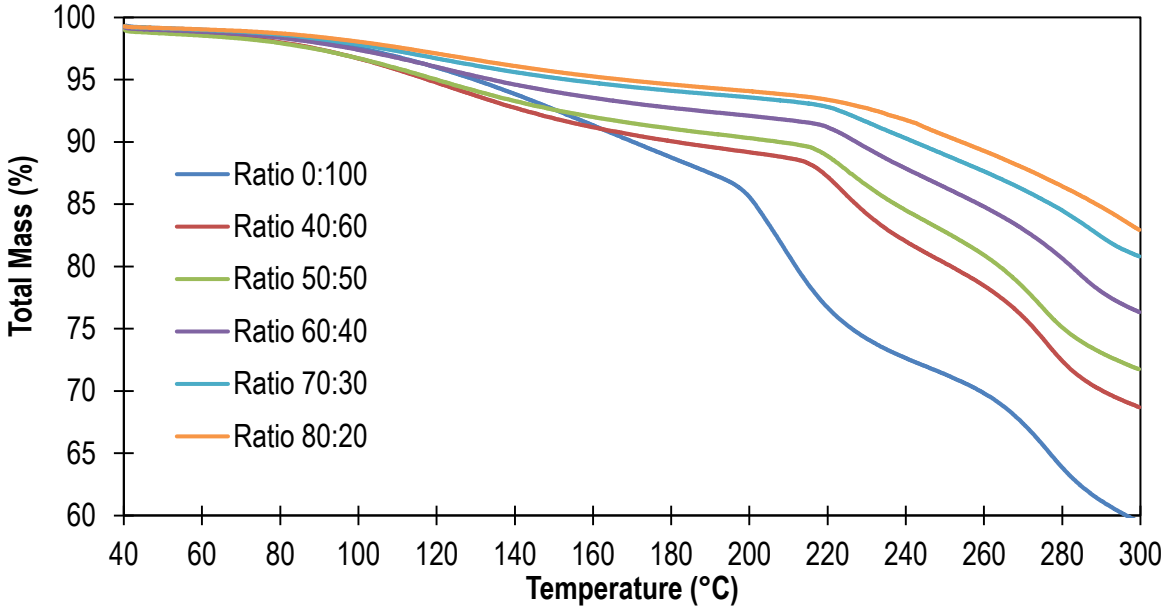

Figure 8 Alginate compartmented fibre at varying rejuvenator/ alginate ratio, TGA results.

Table 5 Total mass lost at 160°C

Ratio	Total mass lost at 160°C (%)
0:100	8.67
40:60	8.82
50:50	8.00
60:40	6.46
70:30	5.25
80:20	4.74

3.3 Healing efficiency of alginate compartmented fibres encapsulating the rejuvenator

3.3.1 microscopic crack healing in bitumen and asphalt mastic

Tabaković et al. [8] reported successful rejuvenator release from the compartmented fibre into artificially induced crack. However, they found that fibres were embedded in the epoxy resin and therefore no crack healing was reported. In this study, in order to investigate rejuvenator release and binder healing the fibres were embedded into the bitumen and artificial cracks were induced into the bitumen and healing efficiency was measured against a control sample without fibres. The fibres of 70:30 (rejuvenator/alginate) ratio were selected for this exercise because in the volumetric analysis, thermal and strength test, they showed to be most suitable fibres for inclusion into the bitumen binder. The healing effect of bitumen with and without the fibres the healing effect of bitumen with and without the fibres is shown in Figure 9 . Figure 9 a – d show healing of a bitumen test sample with fibres. Position of the fibres in the test specimen is marked with a double broken red line. Figure 9 e – h shows healing of a

bitumen test sample without fibre. The test sample with the fibres (Figure 9 a – d) was tested by multi crack healing (3 cracks) in which each crack is induced in order to crack separate fibre compartment encapsulating the bitumen rejuvenator. Figure 9 a and e show undamaged test specimens. Figure 9 b and f show the test specimen immediately after the cracks are induced and the fibre compartments are broken (Figure 9 b). The positions of the cracks in the test specimen are marked with double broken white lines. Figure 9 b shows the rejuvenator release from the compartments into the cracks. Figure 9 c shows healing of all three cracks, containing rejuvenator, 1 hour after the crack insertion. Figure 9 g shows crack healing, of the bitumen test sample without rejuvenator, 3 hours after crack insertion. Both figures show progress in the damage repair, i.e. crack healing. Figure 9 d and h complete damage repair, i.e. crack closure, in both test samples. The results showed bitumen can close the crack (repair the damage) without rejuvenator. However, samples with fibres, i.e. rejuvenator, showed three times faster crack repair (healing). Sample without rejuvenator sealed the crack within 6h where the sample with the fibres (rejuvenator), healed the crack within 2h. These results show that rejuvenator can significantly improve healing ability of the bitumen binders. However, these tests were conducted on the pure bitumen material. In situ, it is expected that the crack will occur in the asphalt mastic (asphalt and fine aggregate mix) [8]. Therefore, it was decided to perform the same test where the healing effect of the encapsulated rejuvenator was tested in the asphalt mastic mix. The information about the asphalt mastic mix design can be found elsewhere [8]. Figure 10 illustrates the healing effect of the alginate fibres encapsulating rejuvenator on the asphalt mastic mix. The position of the fibre in the test sample is marked with double broken red lines and cracks by double broken white line. Figure 10 a shows the test specimen without damage, i.e. cracks. Figure 10 b – d shows test specimen with inserted cracks. Figure 10 b shows rejuvenator release from the fibre compartments into the crack. Figure 10 c and d shows the damage repair, i.e. crack closure, in in the asphalt mastic mix over time. The results show that the self-healing system can repair crack damage, i.e. close the crack, however it does not achieve full crack closure. This finding is in agreement with Garcia et al. [38], who explained that microcapsules, in this case compartmented fibres, cannot fully repair crack damage due to the limited healing agent volume in comparison to the crack volume, however the self-healing system does allow for multiple (partial) crack healing as it is illustrated in the Figure 10, where two cracks are being repaired. Further examination of the crack in ImageJ revealed a volume of the crack is 0,648 μl, whereas a single compartment in the 70:30 fibre contains on an average 0,0162 μl, as shown in Table 4, i.e. 1/40th (2.5%) of the crack volume has been filled with the rejuvenator. Furthermore, in the mastic mix

rejuvenator – bitumen contact surface area is much lower, due to the aggregates, in comparison to the pure bitumen test sample. This indicates that the compartmented fibre self-healing system would perform better within the high bitumen content asphalt mix. These findings show that compartment fibres encapsulating rejuvenator asphalt self-healing system has great potential to repair the crack damage within asphalt pavement system. However, further analysis on a full asphalt pavement mix is required.

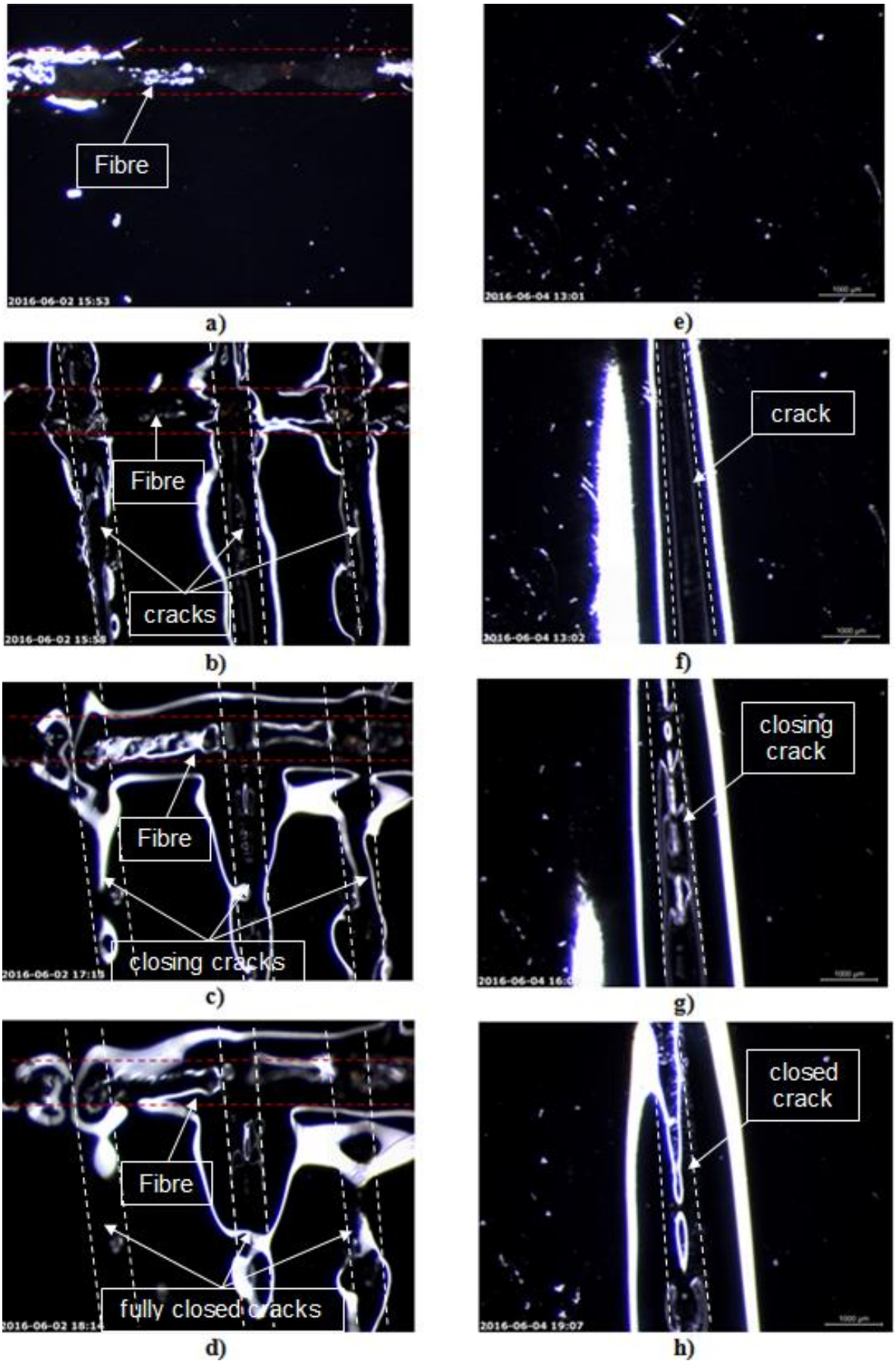

Figure 9 Bitumen crack healing, with (a-d) and without fibres (e-h).

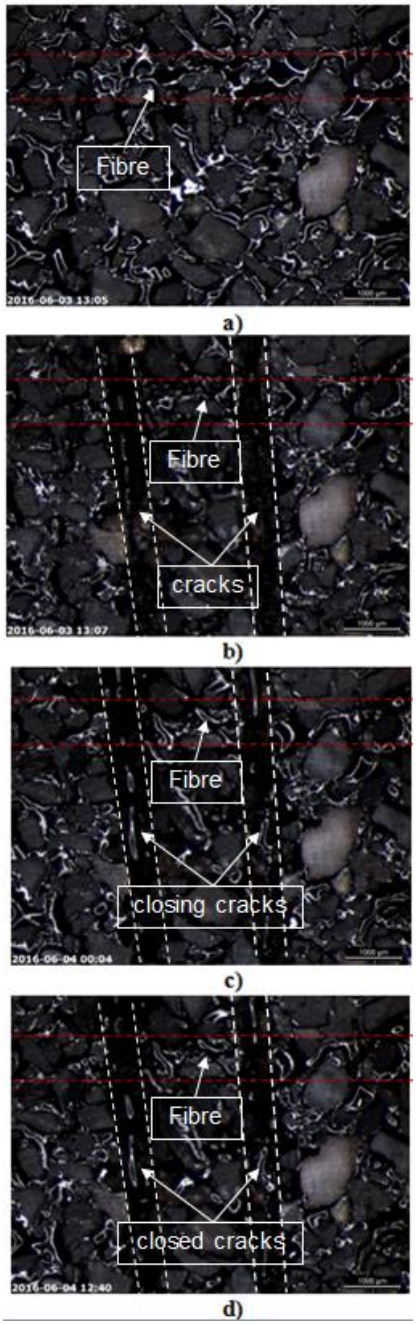

Figure 10 Asphalt mastic crack healing, with fibres (a-d).

3.3.2 Healing efficiency of the compartmented fibres encapsulating rejuvenator self-healing system on the porous asphalt mix.

Following the results from the artificial crack healing experiment, explained above, effect of fibre on the porous asphalt mix stiffness, strength and damage repair (stiffness and strength recovery) has been studied. Figure 11and Figure 12 show the effect of fibres on the stiffness, strength and their healing (strength and stiffness recovery) abilities. The results from the test support authors statement in their previous publication [8] “fibres increase the asphalt mix

strength and stiffness". However, the results from this study show that higher fibre content does not necessarily improve asphalt mix healing properties. From the test results is clear that mixtures with lower amount of fibres (5%) and higher rejuvenator/alginate ratio (70:30) have best ability to recover its original stiffness and strength. The asphalt mixtures with higher fibre content (10%) had lower stiffness and strength recovery, between 10% - 20%. This could be simply due to the fact that fibres once broken cannot be repaired and thus the strength is not recovered. Therefore, samples with higher fibre content experience higher stiffness and strength loss. However, the test sample (asphalt mix) recovery efficiency might have depended on the test sample damage. During the test it was observed that some samples were damaged more than others perhaps this played a role in asphalt mix strength recovery. Therefore, further studies are needed in order to optimise asphalt mix design containing the compartmented alginate fibres encapsulating the bitumen rejuvenator. Nevertheless, these results confirm that compartmented fibres encapsulating the bitumen rejuvenator is viable self-healing technology for asphalt mix crack/damage repair.

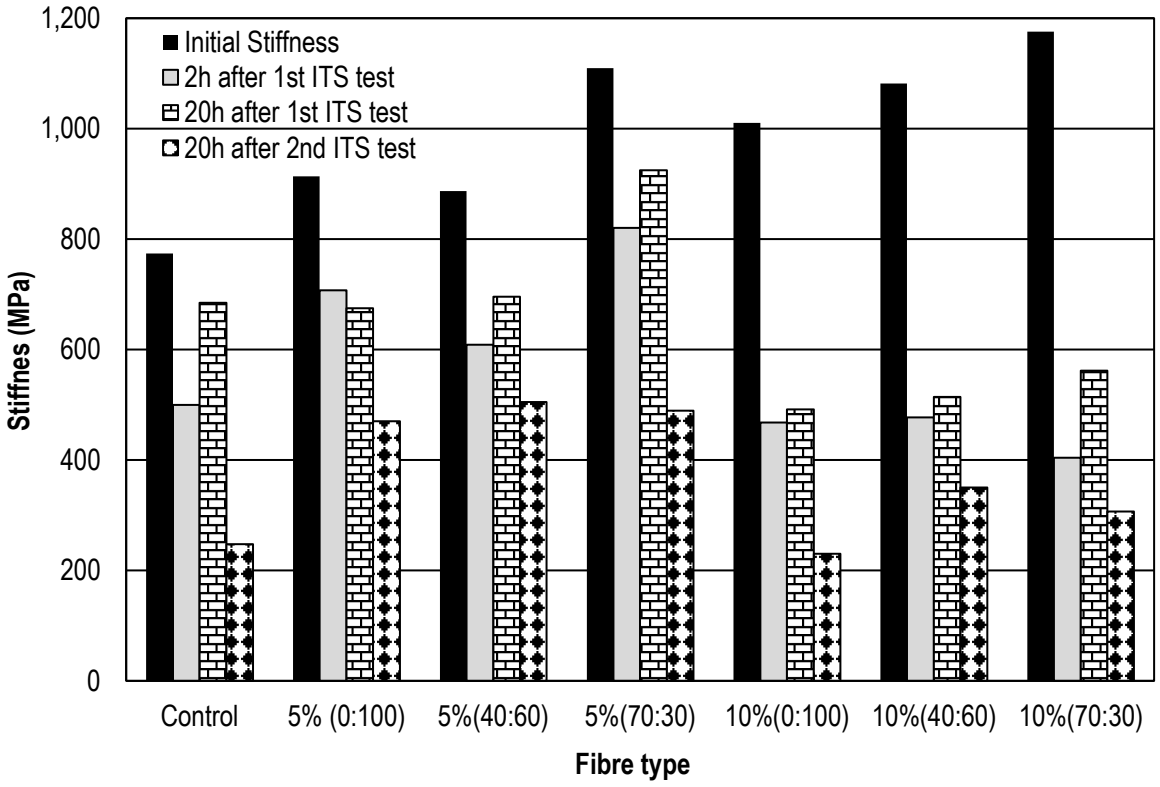

Figure 11 Effect of fibres on asphalt mix stiffness.

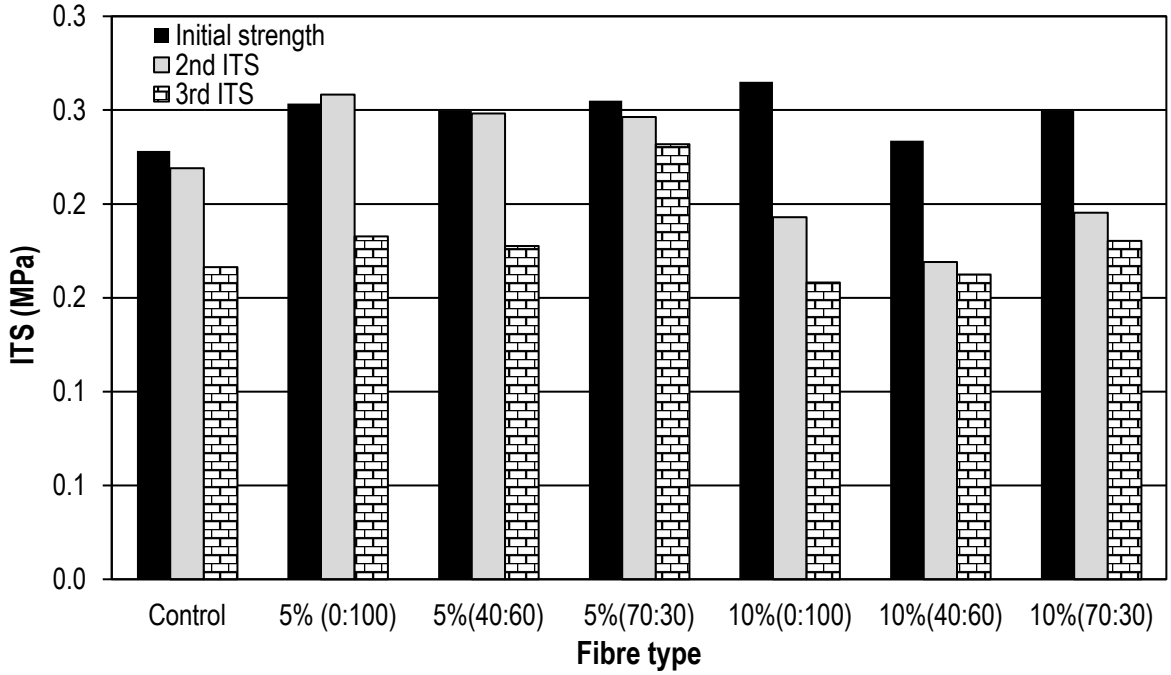

Figure 12 Effect of fibres on asphalt mix strength.

4. Conclusions

The key objective of this study was to optimise design of the compartmented alginate fibre encapsulating rejuvenator, i.e. to determine maximum amount of the rejuvenator that can be encapsulated without compromising the fibre thermal and mechanical properties but improving the system healing efficiency. The results have shown that fibre optimum rejuvenator/alginate ratio is 70:30. This is due to the high volume of the compartments and the stability at different temperatures, while retaining a sufficient mechanical strength for application in asphalt mixes. The results showed that increase in rejuvenator content within the fibre, results in the reduction the fibre mechanical strength. However, the resulting fibre mechanical strength, of the fibres with higher rejuvenator content, is sufficient for its utilisation in asphalt. The fibres will survive the asphalt mixing process and construction and will break due to a crack propagating into the fibre. Insertion of the 70:30 fibres in a bitumen and mastic mix and subsequently introducing artificial cracks demonstrated that the rejuvenator was released from the compartments and filled the crack. Healing of the crack was observed for mixes containing bitumen. The results showed that fibres can increase the bitumen healing rate by three times. However, in an asphalt mastic mix (bitumen and fine aggregate mix) the system has some limited healing capacity. The tip of the crack is sealed, however crack scars are left behind, i.e. full crack healing is not achieved. This is due to the fact that crack volume was 40 times larger than rejuvenator volume released from the

compartment and reduced diffusion area due to the aggregate presence in the asphalt mastic mix. Despite this limitation the system demonstrated that it has the ability to heal the damage as expected, i.e. the tip of the crack is sealed and stress/energy that propagates crack is removed. The study further investigated fibre effect on the ZOAB asphalt mix mechanical properties and self-healing efficiency. The results confirmed earlier findings, that the fibre has good thermal and mechanical strength to survive asphalt mixing and compaction process. The fibre of 70:30 rejuvenator/alginate ratio outperformed the control mix (the mix without fibres) and mixtures containing fibres with lower amounts of rejuvenator. The results also showed that mixtures with higher fibre content have improved initial strength but reduced healing, damage recovery, capacity. The optimisation of the fibre content in the mix will be focus of future work However based on results from this work optimum fibre content in the ZOAB asphalt mix is 5% for compartmented fibres of 70:30 rejuvenator/alginate ratio.

5. Acknowledgements

The authors wish to thank: Dr. Bert Jan Lommerts and Dr. Irina Catiugă, Latexfalt BV, for their support to the project. Authors would also like to thank Mr. Arjan Thijssen for his assistance with the environmental scanning electron microscope. This research was conducted under the Marie Curie IEF research funding, research project Self-healing Asphalt for Road Pavements (SHARP), project number 622863.

6. References

1. Schlangen, E., *Other Materials, Applications and Future Developments*, in *Self-Healing Phenomena in Cement-Based Materials*, M. e Rooij, et al., Editors. 2013, RILEM Series: State-of-the-Art Reports. p. 241 – 256.
2. (OECD), O.o.E.C.a.D., *Road traffic, vehicles and networks*. 2013 in Environment at a Glance 2013: OECD Indicators, OECD Publishing.
3. Vita, L. and M.C. Marolda, *Road Infrastructure – the backbone of transport system*. 2008, EU Directorate General for Research and Sustainable Surface Transport, Brussels, Belgium, EU.
4. European Union Road Federation (ERF), *European road statistics 2012*. 2012: European Union Road Federation Publications.
5. García, A. et al. , *Induction heating of mastic containing conductive fibers and fillers.* Materials and Structures, 2011. **44**(2): p. 499–508.
6. Su, J.F. and E. Schlangen, *Synthesis and physicochemical properties of high compact microcapsules containing rejuvenator applied in asphalt.* Chemical Engineering Journal, 2012. **198-199**: p. 289-300.
7. Hindley, G., *History of Roads*. 1971: The Chaucer Press Ltd.
8. Tabaković, A., et al., *The reinforcement and healing of asphalt mastic mixtures by rejuvenator encapsulation in alginate compartmented fibres.* Smart Materials and Structures, 2016. **25**(8).

9. Tabaković, A., *Recycled Asphalt (RA) for Pavements*, in *Handbook of Recycled Concrete and Demolition Waste*, F. Pacheco-Torgal, et al., Editors. 2013, Woodhead Publishing. p. 394 – 419.
10. Nicholas, J.C., et al. *Effects of using reclaimed asphalt and/or lower temperature asphalt on availability of road network*. in *of 6th International Conference Bituminous Mixtures and Pavements*. 2015. Thessaloniki, Greece.
11. Trombulak, S.C.a.F., C.A., *Review of ecological effects of roads on terrestrial and aquatic communities.* Conservation Biology, 2000. **14**(1): p. 13.
12. Fisher, H., *Self repairing materials – dream or reality.* Natural Science, 2010. **2** (8): p. 873 – 901.
13. García, A., et al., *A simple model to define induction heating in asphalt mastic.* Construction and Building Materials, 2012. **31**: p. 38 - 46.
14. García, A., et al., *Electrical conductivity of asphalt mortar containing conductive fibers and fillers.* Construction and Building Materials, 2009. **21**(10): p. 3175–3181.
15. García, Á., E. Schlangen, and M. van de Ven, *Two ways of closing cracks on asphalt concrete pavements: Microcapsules and Induction Heating.* Key Enginering Materials, 2010. **417-418**: p. 573-576.
16. Su, J.F., J. Qiu, and E. Schlangen, *Stability investigation of self-healing microcapsules containing rejuvenator for bitumen.* Polymer Degradation and Stability, 2013. **98**(6): p. 1205-1212.
17. Su, J.F., et al., *Investigation the possibility of a new approach of using microcapsules containing waste cooking oil; in-situ rejuvenation.* Construction and Building Materials, 2015. **74**: p. 83–92.
18. Su, J.F., et al., *Experimental investigation of self healing behaviour of bitumen/microcapsule composites by modified beam on elastic foundation method.* Materials and Structures, Springer publication, RILEM, 2014.
19. Tabaković, A., et al. *The use of compartmented Sodium-Alginate fibres as healing agent delivery system for asphalt pavements*. in *Proceedings of European Materials Research Society Fall Meeting* 2015. Warsaw, Poland.
20. García, A., *Self-healing of open cracks in asphalt mastic.* Fuel, 2012. **93**: p. 264 – 272.
21. Su, J.F., et al., *Interface stability behaviors of methanol– melamine–formaldehyde shell microPCMs/epoxy matrix composites.* Polymer Composites, 2011. **32**: p. 810–820.
22. Sun, D., et al., *Size optimization and self-healing evaluation of microcapsules in asphalt binder.* Colloid Polymer Science, 2015. **293**: p. 12.
23. Garcia, A., et al., *Internal asphalt mixture rejuvenation using capsules.* Construction and Building Materials, 2015. **101**: p. 8.
24. Garcia, A., et al., *Mechanical properties of asphalt mixture containing sunflower oil capsules.* Journal of Cleaner Production, 2016. **118**: p. 9.
25. Gibney, A., *Analysis of Permanent Deformation of Hot Rolled Asphalt* in *Civil Engineering*. 2002, University College Dublin.
26. Gibney, A. *Prediction of rutting resistance of hot rolled asphalt'*. in *3rd Eurasphalt & Eurobitume Congress*. 2004. Vienna, Austria: Foundation Eurasphalt.
27. Anderson, F.A., *Final Report on the Safety Assessment of Melamine/Formaldehyde Resin.* Journal of the American College of Toxicology, 1995. **14**(5): p. 373-385.
28. Prajer, M., et al., *Direct and indirect observation of multiple local healing events in successively loaded fibre reinforced polymer model composites using healing agent-filled compartmented fibres.* Composites Science and Technology, 2015. **106**: p. 7.

29. Mookhoek, S.D., et al., *Alginate fibres containing discrete liquid filled vacuoles for controlled delivery of healing agents in fibre reinforced composites.* Composites Part A: Applied Science and Manufacturing, 2012. **43**(12): p. 7.
30. Kringos, N., et al., *On the development of a new test methodology for moisture damage susceptibility of asphalt concrete*, in *5th International Conference 'Bituminous Mixtures and Pavements'*. 2011: Thessaloniki, Greece. p. 857 - 867.
31. Tabaković, A., et al, *The influence of recycled asphalt pavement on the fatigue performance of asphalt concrete base courses.* ASCE Journal of Materials in Civil Engineering, 2010. **22**(6): p. 643 - 650.
32. Liu, Q., *Induction healing of porous asphalt concrete*, in *Faculty of Civil Engineering and Geosciences*. 2012, TU Delft, The Netherlands.
33. Kliewer, et al., *Investigation of the relationship between field performance and laboratory ageing properties of asphalt mixtures*, in *Engineering Properties of Asphalt Mixtures and the Relationship to their Performance*, G.A. Huber and D.S. Decker, Editors. 1995.
34. Casado Barrasaa, R., et al., *Addressing durability of asphalt concrete by self-healing mechanism.* Procedia - Social and Behavioral Sciences, 2014. **162**: p. 188.
35. Tabaković, A., et al., *The reinforcement and healing of asphalt mastic mixtures by rejuvenator encapsulation in alginate compartmented fibres.* Smart Materials and Structures, 2016.
36. Schneider, C.A., et al., *NIH Image to ImageJ: 25 years of image analysis.* Nature methods, 2012. **9**(7): p. 5.
37. Doube, M., et al., *BoneJ: Free and extensible bone image analysis in ImageJ.* Bone, 2010. **47**(6): p. 1076-1079.
38. Garcia, S.J. and H.R. Fischer, *Self-healing polymer systems: Properties, synthesis and applications*, in *Smart polymers and their applications*, M. Rosa Aguilar and J. San Roman, Editors. 2014, Woodhead Publishing Limited. p. 271-298.